Thermodynamic assessment of roof-mounted solar process heat for the Mexican denim industry

Eduardo González-Mora[a] and Ma. Dolores Durán-García[a]

[a] *Universidad Autónoma del Estado de México, Toluca, México, egonzalezmo@uaemex.mx, CA*

Abstract:

The decarbonisation of industrial process heat represents one of the most challenging frontiers in the global transition towards low-carbon energy systems, as heat demand accounts for more than half of total industrial energy consumption worldwide. Parabolic trough collector (PTC)-based Solar Heat for Industrial Processes (SHIP) has emerged as a technically mature pathway for supplying medium-temperature process heat from renewable sources, yet its deployment in space-constrained existing facilities remains largely uncharacterised. In the textile manufacturing sector, where steam demand is continuous and rooftop installation area is severely limited, no prior study has rigorously assessed the thermodynamic feasibility of PTC-based SHIP using an exergy-centred framework under realistic spatial constraints. Here we show that roof-mounted PTC systems integrated with thermocline thermal energy storage can achieve solar fractions of 31.6–33.4% and displace 50–83% of annual natural gas consumption in denim manufacturing facilities within the Toluca Valley, México, operating within a rooftop envelope of less than 931 m² per factory. These results advance the existing literature by delivering the first exergy-focused, area-constrained assessment of PTC-based SHIP for the Mexican textile industry, revealing time-averaged second-law efficiencies of 20.0–25.8% and demonstrating that the exergy-based solar fraction diverges systematically from its energy-based counterpart—a distinction that energy-only analyses consistently overlook. We further demonstrate that heat exchanger temperature mismatching and thermocline storage degradation constitute the dominant sources of thermodynamic irreversibility, identifying these components as primary targets for future performance improvement. The validated, non-iterative thermohydraulic modelling framework and constrained-area sizing methodology developed in this work provide a replicable design tool applicable to industrial solar heat integration in space-limited facilities across Latin America and other emerging economies pursuing industrial decarbonisation.

Keywords:

Solar heat for industrial processes; PTC; Exergy analysis; Industrial decarbonization.

1. Introduction

Industrial decarbonisation represents a critical global imperative, as industrial activities account for a substantial portion of energy consumption and greenhouse gas emissions. This reality demands an urgent transition toward low-carbon heat sources. Process heat lies at the heart of this challenge, accounting for approximately 70% of the industrial sector's energy input worldwide across low-, medium-, and high-temperature ranges [1,2]. The industrial sector consumes roughly 30% of global energy and generates between 28% and 39% of CO^2 emissions, with process heat constituting the primary contributor [1,2]. Despite the urgency, renewable penetration in industrial heat remains stubbornly low—far below the levels required to meet net-zero targets. Most industrial heat continues to rely on fossil fuels such as natural gas and coal. While solar and other renewable technologies expand rapidly in the electricity sector, their share in dispatchable industrial heat provision remains minimal. Even under optimistic scenarios, projections indicate a potential uptake of only 10% to 28% in specific applications, such as food processing, by 2035 [2]. Decarbonising hard-to-abate industries requires a portfolio of solutions. These include waste heat recovery, electrification via high-temperature heat pumps, and the integration of renewable technologies using concentrating solar thermal (CSP) systems. Crucially, CSP technologies can integrate directly with existing industrial plants, minimising operational disruptions while leveraging brownfield sites and modular system architectures. Such approaches offer viable pathways toward net-zero emissions by 2050 [3].

Solar Heat for Industrial Processes (SHIP) employs solar thermal collectors to supply clean thermal energy to industry, with systems categorised by temperature ranges that align with specific process requirements. As of late 2024, global SHIP deployment exceeded 1 GWth across more than 1300 installed systems [4]. Textile manufacturing depends heavily on thermal energy across multiple production stages. Washing requires

temperatures of 60–90°C, bleaching operates at 80–100°C, dyeing demands 100–140°C, drying requires 120–180°C, and ironing or thermo-fixing necessitates 150–200°C. Collectively, these processes account for 60–80% of the sector's energy consumption, primarily in the form of steam or hot water derived from fossil fuels [5]. Several international case studies demonstrate the viability of SHIP in textile applications. In India, a 2210 m^2 parabolic trough collector (PTC) system at a textile facility in Rajasthan supplies steam at 180°C, saving 1200 MWh annually and reducing CO_2 emissions by 1000 tonnes per year. China's Shandong province hosts a pilot project employing linear Fresnel collectors for dyeing operations, which achieving 25% fuel displacement. Mediterranean installations include a Moroccan retrofit using flat-plate collectors that delivers 70°C water for washing processes, with a payback period of under four years [4,6].

Existing studies rarely address space-constrained, roof-mounted SHIP retrofits in densely populated urban industrial zones, a gap that limits the scalability of solar thermal integration. Furthermore, exergy-based assessments remain scarce in the literature, leading researchers to overlook efficiency losses beyond simple energy input accounting. Critically, data for México remains absent from the SHIP knowledge base, despite the country's high solar potential and established textile manufacturing hubs in Puebla, Hidalgo, and the Toluca Valley [4,7,8]. México's industrial sector relies heavily on natural gas, faces escalating fuel costs, and benefits from policies that actively promote renewable energy adoption amid a national push for energy transition. The textile industry constitutes a key economic driver, concentrated in central regions where solar resources present a strategic opportunity for SHIP deployment [8,9].

Textiles contribute approximately 1.5% to 2% of México's GDP, representing an annual value of US$10–12 billion. The sector employs more than 400,000 workers and generates exports exceeding US$5 billion, primarily destined for the USMCA bloc. Key production hubs include the Toluca Valley in the Estado de México, which accounts for 25% of national output; the Puebla-Tlaxcala region, contributing 35%; and the states of Hidalgo and Guanajuato. These areas host numerous wet-processing plants that rely on gas-fired boilers for 70% of their energy requirements. Current practice favours natural gas, which holds a 60% to 80% share in steam generation, while electrification remains low and renewable integration rare due to high upfront capital costs [10,11].

Central México boasts excellent solar potential for industrial applications. Annual Global Horizontal Irradiance (GHI) ranges from 5.5 to 6.2 kWh/m^2/day, while Direct Normal Irradiance (DNI) reaches 1900 to 2200 kWh/m^2/year—values ideal for parabolic trough and linear Fresnel SHIP systems. DNI maps reveal peaks exceeding 2.3 kWh/m^2/day during dry seasons, supporting 1800 to 2000 full-load operating hours annually for medium-temperature applications. This resource significantly exceeds European averages, enabling payback periods of under five years for textile industry retrofits [8,12].

Despite growing interest in Solar Heat for Industrial Processes (SHIP), a critical gap persists in the literature: no prior study has rigorously evaluated the thermodynamic feasibility of parabolic trough collector (PTC)-based SHIP systems under the spatial constraints characteristic of existing textile manufacturing facilities. In the Toluca Valley, where the denim industry represents a significant share of regional industrial energy demand, factories face the compounded challenge of decarbonising high-temperature process heat while operating within severely limited rooftop installation areas. Conventional techno-economic assessments routinely neglect this spatial constraint. Furthermore, existing SHIP studies for the Mexican industrial sector rarely adopt an exergy-based framework. Such a framework is essential for identifying the true thermodynamic irreversibilities that limit system performance and for guiding meaningful efficiency improvements.

To address these gaps, this work presents the first exergy-focused assessment of roof-mounted PTC systems tailored to Mexican denim manufacturing. We integrate real site-specific meteorological data, validated component models, and a constrained-area optimisation procedure applied across two representative factories in the Toluca Valley. Through this approach, we deliver a rigorous evaluation of the technical, thermodynamic, and environmental performance of a SHIP system operating under realistic industrial boundary conditions in central Mexico.

2. Methodology

2.1. Case study description

We selected two representative sites within the Toluca Valley of central México for analysis, reflecting the regional concentration of denim manufacturing activity. The first site lies in the city of Toluca (19.29° N, 99.65° W) and the second in Almoloya del Río (19.16° N, 99.49° W). We chose these locations based on the significant and growing presence of textile and denim facilities throughout the valley. This clustering pattern amplifies the collective demand for industrial process heat and therefore strengthens the case for evaluating a replicable, area-constrained SHIP solution applicable across multiple co-located factories.

The industrial process under analysis encompasses the washing and ironing operations common to denim manufacturing, both of which require saturated steam at 6 bar. Each factory demands 648 kg/h of steam, with feedwater supplied at 20°C. This demand yields a net thermal power requirement ($\dot{Q}_{\mathrm{load}}$) of 477.1 kW and a

daily energy demand of 7.63 MWh. Based on an operating schedule of 16 hours per day across 305 working days in 2025—accounting for all official non-working days as detailed in Table 1—the annual thermal energy demand per facility amounts to 2328 MWh.

At present, each factory meets this demand entirely by combusting natural gas in a fire-tube boiler operating at a thermal efficiency of 87.8%. This configuration consumes 597.1 kg of fuel per day, equivalent to 182.1 tonnes per year. The associated annual fuel expenditure, calculated using the monthly natural gas tariffs reported in Table 1, totals US$673,525 per factory.

Regarding the potential for solar integration, each factory offers a rooftop area of 49 m × 19 m, yielding a gross surface of 931 m^2. However, the effective area available for collector deployment necessarily reduces once we make provisions for inter-row shading avoidance, maintenance corridors, and structural constraints. Because of these spatial limitations, the solar system cannot satisfy the full thermal demand. Consequently, we must assess the SHIP configuration as a partial-substitution solution operating under a constrained-area regime.

Table 1. *Facility month data [13].*

Month	Working days	Natural gas cost, (USD/kg)
January	26	4.2
February	23	3.9
March	25	3.3
April	25	3.8
May	26	3.4
June	25	3.6
July	27	3.6
August	26	3.3
September	25	3.4
October	27	3.4
November	24	4.5
December	26	4.0

2.2. Solar thermal system design

The proposed SHIP system employs Therminol VP-1 as the heat transfer fluid (HTF). We selected this fluid for its well-documented thermal stability at operating temperatures up to 400°C [14], its compatibility with parabolic trough systems, and its favourable safety profile within enclosed rooftop installations. In the present configuration, the HTF circulates between an inlet temperature of 140°C and an outlet temperature of 240°C. This temperature range ensures adequate thermal driving force for steam generation whilst remaining within the validated operating envelope of the selected fluid.

The collector array comprises PT250 Power Trough units, a small-aperture parabolic trough model specifically optimised for industrial-scale integration in the Mexican market [15]. We selected this collector based on its commercial availability in México, its rated temperature capability of up to 250°C, and its demonstrated performance under conditions representative of the study region.

Thermal energy transfer between the solar HTF loop and the facility's existing steam header occurs through a shell-and-tube heat exchanger configured in a one-shell-pass, two-tube-pass arrangement. We chose this configuration for its efficiency in handling the temperature differentials characteristic of this application.

To mitigate the effects of solar intermittency and enhance overall system reliability, the installation incorporates a centralised thermocline thermal energy storage unit with a two-hour capacity. This unit employs Therminol VP-1 as the sensible storage medium and operates with a solar multiple (SM) of 1.5. This configuration buffers fluctuations in solar irradiance, maintains a more consistent steam supply to the process headers, and reduces reliance on auxiliary natural gas firing during periods of partial cloud cover or transient irradiance loss. Table 2 summarises the key operating specifications of the system, and Figure 1 presents a schematic layout of the proposed installation.

Table 1. *Parabolic trough collector PT250 specifications [15].*

Parameter	Symbol	Value
Width, (m)	W	2.5
Focal length, (m)	f	0.930
Aperture area, (m^2)	A_{ap}	10
Outer receiver diameter, (m)	d_{out}	0.040

Inner receiver diameter, (m)	d_{in}	0.037
Glass cover outer diameter, (m)	$d_{\mathrm{c,out}}$	0.0572
Glass cover inner diameter, (m)	$d_{\mathrm{c,in}}$	0.0542
Peak optical efficiency	$\eta_{\mathrm{o,max}}$	0.7464

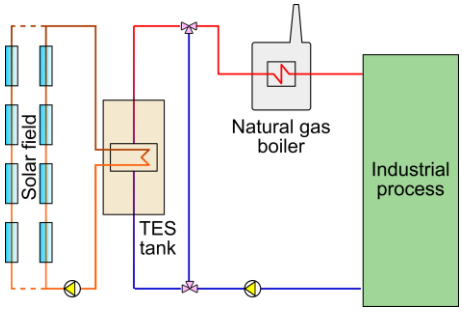

Figure. 1. *Schematic diagram of the solar thermal installation.*

2.3. Thermodynamic model framework

The proposed SHIP system integrates a PTC solar field, a single-node thermocline TES unit, and a shell-and-tube heat exchanger (HX). The natural gas boiler operates in series as an auxiliary heat source. We evaluate system performance using a validated, non-iterative thermohydraulic model coupled with comprehensive energy (first law) and exergy (second law) analyses conducted on an hourly basis throughout the year.

The model comprises a validated thermohydraulic routine that tracks the temperature and pressure evolution of the Therminol VP-1 HTF as it flows through the solar field. To characterise PTC performance, we segment each receiver tube into discrete heat collector elements (HCEs). This discretisation strategy enables precise accounting of incident beam solar irradiation, optical losses, thermal losses to the environment, and the resultant enthalpy gain of the HTF along the flow path. The model has undergone validation against experimental data, demonstrating predictive robustness with a relative squared error (RSE) below 3% for both temperature and pressure calculations across the operating range of interest [16].

A key methodological contribution of the thermohydraulic routine lies in its elimination of the traditional iterative dependency on convective heat transfer coefficients and friction factors. We achieve this by integrating established Nusselt and friction correlations through functional transformations that render the governing equations separable in terms of the primary variable functionals, expressed as $\dot{q}' = f(\Delta T)$ [16]. This reformulation decouples the thermal and hydraulic sub-problems, substantially enhancing computational efficiency whilst preserving physical fidelity. The governing energy balance for a single HCE, which accounts for all relevant heat fluxes illustrated in Figure 2, takes the form:

$$\begin{cases} \dot{q}_{i,\mathrm{SolAbs}} = IAM\eta_{\mathrm{o,max}} W G_{\mathrm{bn}} \\ \dot{q}_{i,\mathrm{cond}} = \frac{2\pi k_{ij}\left(T_i - T_j\right)}{\ln d_j/d_i} \\ \dot{q}'_{i,\mathrm{rad}} = \frac{\sigma\pi d_i\left(T_i^4 - T_j^4\right)}{\frac{1}{\varepsilon_i} + \frac{\left(1-\varepsilon_j\right)d_i}{\varepsilon_j d_j}} \\ \dot{q}'_{i,\mathrm{conv}} = f(\Delta T) \end{cases}, \qquad (1)$$

where IAM is the incidence angle modifier is determined via raytracing, G_{bn} is the direct normal irradiance (DNI), k is thermal conductivity, T is temperature, d is diameter, σ is the Stefan-Boltzmann constant, and ε is emittance. The net energy balance for a PTC module of length L is:

$$\dot{Q}_{\mathrm{PTC}} = \dot{Q}_{\mathrm{in}} - \dot{Q}_{\mathrm{loss}} = A_{\mathrm{c}} G_{\mathrm{bn}} \eta_{\mathrm{o,max}} F_{\mathrm{soil}} IAM - \dot{Q}_{\mathrm{loss}}, \qquad (2)$$

where A_{c} is the collector aperture area, F_{soil} is a soiling factor (0.92 in this study), and $\dot{Q}_{\mathrm{loss}}$ represents the conductive, convective and radiative losses in the receiver, as shown in Figure 2.

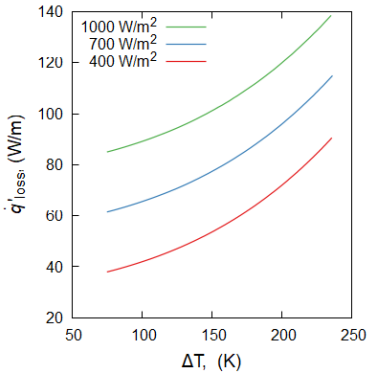

Figure. 2. *Thermal losses for the PT250 collector.*

We size the solar field based on the available rooftop area of 931 m^2, applying an inter-row spacing equal to twice the collector aperture width. We selected this spacing value to suppress row-to-row shading at the winter solstice whilst maintaining a reasonable land-use factor within the established range of 1.2 to 2.0 times the aperture width. Under this spatial constraint, we design the solar field to supply a fraction K of the total process thermal load $\dot{Q}_{\text{load}}$, such that the nominal solar contribution becomes $\dot{Q}_{\text{nom,sun}} = K\dot{Q}_{\text{load}}$. One defines the solar multiple ($SM > 1$) s the ratio of the designed solar field thermal output $\dot{Q}_{\text{des}}$ to this nominal solar contribution $\dot{Q}_{\text{nom,sun}}$:

$$SM = \frac{\dot{Q}_{\text{des}}}{\dot{Q}_{\text{nom,sun}}} = \frac{\dot{m}_{\text{SF}} c_{p,\text{HTF}} \Delta T_{\text{HTF}}}{K\dot{Q}_{\text{load}}} \qquad (3)$$

where $\dot{m}_{\text{SF}}$ represents the total HTF mass flow rate through the field, $c_{p,\text{HTF}}$ denotes the fluid's specific heat capacity, and ΔT_{HTF} is the design temperature rise across the collector array. We set the HTF flow rate per collector loop to maintain a fully turbulent regime, from which we subsequently determine the number of parallel loops N_{loops} and the total number of collectors $N_{\text{PTC,tot}}$. We fix the design point at solar noon on the spring equinox, a conservative reference condition that ensures a minimum guaranteed thermal output from the SHIP system throughout the year.

We size the TES unit to store surplus thermal energy accumulated during periods of peak solar irradiation. To calculate the required storage volumen V_{TES}, we use the desired storage duration $t_{\text{storage}} = 2\,\text{h}$ and the volumetric thermal energy density of the HTF:

$$V_{\text{TES}} = \frac{\dot{Q}_{\text{nom,sun}} t_{\text{storage}}}{\rho_{\text{HTF}} c_{p,\text{HTF}} \Delta T_{\text{HTF}}} \qquad (4)$$

We conduct a time-resolved hourly simulation to determine both the instantaneous and period-integrated performance of the integrated system. The dispatch logic follows a strict priority sequence: direct solar use takes precedence, followed by thermal energy storage discharge to cover any remaining deficit. The natural gas boiler then supplies any load that neither the solar field nor the storage unit can meet. We define the instantaneous total energy efficiency of the system $\eta_{\text{I,tot}}$ as the ratio of useful thermal energy delivered to the process to the total primary energy input from all contributing sources:

$$\eta_{\text{I,tot}}(t) = \frac{\dot{Q}_{\text{process}}(t)}{\dot{Q}_{\text{sun}}(t) + \dot{Q}_{\text{fuel}}(t)} \qquad (5)$$

where $\dot{Q}_{\text{sun,in}} = G_{\text{bn}}(t)\, A_{\text{tot}}$ represents the solar power intercepted by the PTC array, and $\dot{Q}_{\text{fuel}} = \dot{m}_{\text{fuel}}(t)\text{LHV}$ denotes the thermal power contributed by the auxiliary fuel. The total useful thermal energy delivered to the process, $\dot{Q}_{\text{process}}$, comprises three distinct contributions:

$$\dot{Q}_{\text{process}}(t) = \dot{Q}_{\text{s,direct}} + \dot{Q}_{\text{TES,dis}} + \dot{Q}_{\text{fuel}} \qquad (6)$$

where $\dot{Q}_{\text{s,direct}}$ the direct solar contribution, produced by the solar field and delivered immediately to the heat exchanger, $\dot{Q}_{\text{TES,dis}}$ the stored solar contribution, representing surplus thermal energy diverted to the TES unit and subsequently retrieved during discharge periods; and $\dot{Q}_{\text{fuel}}$ is he auxiliary contribution, supplied by the natural gas boiler when solar resources prove insufficient to meet the process load. The direct solar contribution is derived from the solar field energy efficiency, accounting for the incident solar input $\dot{Q}_{\text{sun,in}}$:

$$\dot{Q}_{\text{s,direct}} = \eta_{\text{I,SF}} \dot{Q}_{\text{sun,in}} \qquad (7)$$

$$\eta_{\text{I,SF}} = \frac{\dot{Q}_{\text{gain,HTF}}}{\dot{Q}_{\text{sun,in}}} = \frac{\dot{m}_{\text{SF}}(h_{\text{out}} - h_{\text{in}})}{G_{\text{bn}} A_{\text{tot}}} \qquad (8)$$

The auxiliary boiler supplies the remaining unmet load. We calculate this useful heat output from the boiler's thermal efficiency $\eta_{\text{I,boiler}}$and its instantaneous fuel mass flow rate:

$$\dot{Q}_{\text{fuel}} = \eta_{\text{I,boiler}} \dot{m}_{\text{fuel}} LHV \qquad (9)$$

The shell-and-tube heat exchanger transfers thermal energy from the HTF loop to the process steam header. Consequently, both $\dot{Q}_{\mathrm{s,direct}}$ and $\dot{Q}_{\mathrm{TES,dis}}$ incorporate the heat exchanger energy efficiency $\eta_{\mathrm{I,HX}}$ when delivering useful heat to the process. This approach ensures consistent thermodynamic accounting across the solar field, storage unit, and process load. We derive the heat exchanger energy efficiency from its number of transfer units (NTU) and heat capacity rate ratio $\dot{C}_{\mathrm{r}} = \dot{C}_{\min}/\dot{C}_{\max}$ [17]:

$$\eta_{\mathrm{I,HX}} = \frac{1}{NTU}\frac{1}{\frac{1}{\varepsilon_{\mathrm{HX}}}-\frac{1+\dot{C}_{\mathrm{r}}}{2}} \quad (10)$$

The exergy analysis quantifies the thermodynamic quality of all energy flows within the system. We express the specific physical exergy of the HTF using the standard formulation $\psi_{\mathrm{HTF}} = c_{p,\mathrm{HTF}}[(T-T_0) - T_0\ln(T/T_0)] + v(P-P_0)$,where T_0 represents the ambient (dead-state) temperature and v denotes the specific volume of the fluid. We evaluate the exergy input from solar radiation using the endoreversible MPD model [18]. For the natural gas chemical exergy, we employ Szargut's correlation $ex_{\mathrm{ch}} = \phi LHV$, where $\phi = 0.92$ for natural gas [19]. he exergy supplied by the fuel therefore becomes $\dot{E}x_{\mathrm{fuel}} = \dot{m}_{\mathrm{fuel}} ex_{\mathrm{ch}}$. We define the exergy efficiencies of the solar field and the heat exchanger respectively as:

$$\eta_{\mathrm{II,SF}} = \frac{\dot{m}_{\mathrm{SF}}\Delta\psi_{\mathrm{HTF}}}{\dot{E}x_{\mathrm{sun}}} \quad (11)$$

$$\eta_{\mathrm{II,HX}} = \frac{\dot{m}_{\mathrm{load}}\Delta\psi_{\mathrm{load}}}{\dot{m}_{\mathrm{SF}}\Delta\psi_{\mathrm{HTF}}} \quad (12)$$

The instantaneous total exergy efficiency of the integrated system is:

$$\eta_{\mathrm{II,tot}}(t) = \frac{\dot{E}x_{\mathrm{process}}(t)}{Ex_{\mathrm{sun}}(t)+\dot{E}x_{\mathrm{fuel}}(t)} \quad (13)$$

where $\dot{E}x_{\mathrm{process}}$ represents the total exergy rate delivered to the process. This total comprises three distinct contributions: $\dot{E}x_{\mathrm{s,direct}}$, the exergy rate from direct solar heat, which we obtain by applying the physical exergy formulation to $\dot{Q}_{\mathrm{s,direct}}$; $\dot{E}x_{\mathrm{TES,dis}}$, the exergy rate from TES discharge, which we evaluate for heat delivered at temperature T_{HTF} as $\dot{E}x_{\mathrm{TESmdis}} = \dot{Q}_{\mathrm{TES,dis}}(1 - T_0/T_{\mathrm{HTF}})$; and $\dot{E}x_{\mathrm{fuel,out}}$, the exergy contribution from the auxiliary boiler, which accounts for its exergy efficiency. Both $\dot{E}x_{\mathrm{s,direct}}$ and $\dot{E}x_{\mathrm{TES,dis}}$ incorporate the heat exchanger exergy efficiency when transferring exergy from the HTF loop to the process.

We employ several complementary metrics to assess system performance on an annual basis. These metrics collectively characterise the energy balance, exergetic quality, fuel savings, component utilisation, and overall thermodynamic performance of the installation. The solar fraction (SF) quantifies the proportion of the total process heat demand satisfied by solar-derived sources, encompassing both direct PTC output and thermal energy storage discharge:

$$SF = \frac{Q_{\mathrm{s,direct}}+Q_{\mathrm{TES,dis}}}{Q_{\mathrm{process}}} \quad (14)$$

where $Q_{\mathrm{s,direct}}$ represents the cumulative useful energy delivered directly by the collectors, $Q_{\mathrm{TES,dis}}$ denotes the cumulative energy discharged from the TES unit, and Q_{process} is the total process energy demand over the accounting period. A higher solar fraction indicates greater displacement of auxiliary fuel. However, achieving very high solar fraction values typically entails disproportionate increases in collector area and storage capacity, which may compromise both the spatial feasibility and economic viability of the installation.

Whilst the conventional solar fraction addresses energy quantity, the exergy-based solar fraction (SF_{ex}) provides a complementary assessment of energy quality. This metric expresses the solar and storage exergy contributions relative to the total exergy demand of the process:

$$SF_{\mathrm{ex}} = \frac{Ex_{\mathrm{s,direct}}+Ex_{\mathrm{TES,dis}}}{Ex_{\mathrm{process}}} \quad (15)$$

where $Ex_{\mathrm{s,direct}}$ and $Ex_{\mathrm{TES,dis}}$ represent the cumulative exergy delivered by the collectors and the TES unit respectively, and Ex_{process} denotes the total exergy required by the process. Both terms incorporate the heat exchanger exergy efficiency when transferring exergy from the HTF loop to the steam header. This formulation recognises that thermal energy at different temperatures carries different capacity for performing useful work, and therefore provides a more rigorous thermodynamic evaluation of the solar system's contribution. The fuel saved fraction (FSF) quantifies the reduction in auxiliary fuel consumption relative to a boiler-only baseline:

$$FSF = \frac{E_{\mathrm{fuel,base}}-E_{\mathrm{fuel}}}{E_{\mathrm{fuel,base}}} \quad (16)$$

where $E_{\mathrm{fuel,base}}$ represents the fuel energy consumed in the reference boiler-only scenario, and E_{fuel} denotes the fuel energy consumed by the auxiliary boiler in the solar-assisted configuration. This metric directly reflects the fossil fuel displacement achieved through solar integration, along with the associated reductions in operating costs and carbon emissions. The capacity factor (CF) measures the degree to which the installed solar infrastructure contributes useful energy relative to its theoretical maximum. We define this factor as the ratio of the actual annual energy output from the solar field to the theoretical maximum output achievable under continuous operation at rated capacity:

$$CF = \frac{E_{\mathrm{SF}}}{\dot{Q}_{\mathrm{des}}\Delta t} \quad (17)$$

where E_{SF} represents the actual energy output from the solar field over the period Δt. A high-capacity factor indicates consistent and intensive utilisation of the collector array, which improves the return on the capital invested. Finally, we assess the overall thermodynamic performance of the system through time-averaged energy and exergy efficiencies. These metrics integrate the respective instantaneous values over the full annual operating period. We define the time-averaged total energy efficiency as:

$$\bar{\eta}_{\mathrm{I,tot}} = \frac{\int_0^t \dot{Q}_{\mathrm{process}}(t)\mathrm{d}t}{\int_0^t [\dot{Q}_{\mathrm{sun}}(t)+\dot{Q}_{\mathrm{fuel}}(t)]\mathrm{d}t} \quad (18)$$

and the time-averaged total exergy efficiency as:

$$\bar{\eta}_{\mathrm{II,tot}} = \frac{\int_0^t \dot{E}x_{\mathrm{process}}(t)\mathrm{d}t}{\int_0^t [\dot{E}x_{\mathrm{sun}}(t)+\dot{E}x_{\mathrm{fuel}}(t)]\mathrm{d}t} \quad (19)$$

These integrated metrics serve as robust, single-figure indicators of the system's cumulative capacity to convert incoming energy and exergy resources into useful process heat delivery. They account for the combined effects of part-load operation and transient conditions throughout the year.

3. Results and discussion

In this section, we present and interpret the thermodynamic and energetic performance of the proposed roof-mounted, PTC-based SHIP system for the two factory sites under analysis: Almoloya del Río and Toluca. We discuss results in terms of solar field sizing, energy and exergy performance, fuel displacement, and operational cost savings. Where appropriate, we draw cross-site comparisons to contextualise the influence of local meteorological conditions on system behaviour. Table 3 consolidates the principal performance indicators for both sites to facilitate direct comparison.

Table 3. *Summary of key performance indicators for the Almoloya del Río and Toluca factory sites.*

Parameter	Almoloya del Río	Toluca
Total PTC collectors	44	
Concentrating area, (m^2)	440	
Nominal solar contribution, (kW)	109.7	143.1
Real solar multiple	1.553	1.653
TES volume, (m^3)	4.2335	5.524
Thermal load fraction, K	0.23	0.30
Pressure drop, (bar)	0.048	0.081
Direct solar delivery, (MWh)	257.149	315.118
Solar fraction, SF (%)	33.4	31.6
Exergy based solar fraction, SF_{ex} (%)	37.9	29.5
Capacity factor	0.318	0.299
Fuel saved fraction, FSF (%)	50	83.1
Average energy efficiency, $\bar{\eta}_{\mathrm{I,tot}}$	0.635	0.655
Average exergy efficiency, $\bar{\eta}_{\mathrm{II,tot}}$	0.200	0.258
Annual fuel consumption – baseline, (ton)	54.59	54.99
Annual fuel consumption – solar assisted, (ton)	27.359	9.3
Annual fuel cost – baseline, (USD)	8174.24	
Annual fuel cost – solar-assisted, (USD)	4119.32	1415.11
Annual cost saving, (USD)	4054.92	6759.13

Both sites accommodate an identical collector array comprising 44 PT250 parabolic trough collectors distributed across two parallel loops of 22 units each. This configuration yields a total concentrating aperture area of 440 m^2 and requires an installation footprint of 880 m^2. The layout remains consistent with the rooftop constraint of 931 m^2 established in the methodology and confirms that the proposed arrangement is spatially feasible under the inter-row spacing criterion of twice the aperture width. The pressure drop across the solar field is 0.048 bar at Almoloya del Río and 0.081 bar at Toluca. The marginally higher value at Toluca arises from its greater nominal solar contribution of 143.1 kW, compared with 109.7 kW at Almoloya del Río. The realised solar multiples are 1.553 and 1.563 respectively, both closely consistent with the design target of 1.5. This agreement confirms that the sizing procedure outlined in the methodology produces reliable results under the spatial constraints of this study. The thermal energy storage volumes are 4.235 m^3 for Almoloya del Río

and and 5.524 m^3 for Toluca, reflecting the proportionally larger storage requirement associated with the higher nominal output at the Toluca site. The thermal load fraction K—representing the share of the process load nominally assignable to the solar field under design conditions—is 0.23 for Almoloya del Río and 0.30 for Toluca. These values underscore that the area constraint prevents full solar coverage of process demand at either site. Consequently, the system must operate in partial-substitution mode, precisely as anticipated in the methodology.

The annual energy results reveal meaningful differences between the two sites, driven primarily by their distinct solar resource characteristics. At Almoloya del Río, the solar field delivers 257.149 MWh of direct solar heat to the process annually, supplemented by 12.417 MWh discharged from the thermal energy storage unit. Together, these contributions satisfy a solar fraction of 33.4% of the total annual process demand of 808.215 MWh. At Toluca, direct solar delivery amounts to 315.118 MWh, with an additional 18.094 MWh from TES discharge. These contributions yield a solar fraction of 31.6% against a higher annual process demand of 1054.289 MWh. The higher absolute solar output at Toluca is attributable to the greater nominal design point, though the correspondingly larger process demand tempers the resulting solar fraction relative to Almoloya del Río.

The capacity factor is 0.318 at Almoloya del Río and 0.299 at Toluca, indicating that the collector array at both sites operates at approximately 30% of its theoretical maximum continuous output. These values are consistent with expectations for a rooftop-constrained PTC installation in central Mexico operating across 305 days per year with a 16-hour daily schedule. They reflect the combined effect of nocturnal non-operation, cloud cover, and seasonal irradiance variation. The TES contribution, whilst modest in absolute terms, plays an important role in buffering transient solar deficits and marginally extending the daily solar supply window beyond direct collection hours.

Figures 3a and 3b present heatmaps illustrating the hourly and seasonal distribution of direct solar heat delivery $\dot{Q}_{\mathrm{s,direct}}$ for Almoloya del Río and Toluca respectively. Both figures reveal a pronounced concentration of thermal output during the central hours of the day, particularly between approximately 09:00 and 15:00. Maximum values occur in the spring and early summer months when beam normal irradiance is highest and the solar angle most favourable. The winter months exhibit noticeably lower and more temporally compressed output windows, consistent with the reduced solar altitude and shorter daylight periods characteristic of the Toluca Valley at this latitude. A comparison of the two heatmaps confirms that the Toluca site sustains marginally higher peak hourly outputs, consistent with its larger nominal design contribution.

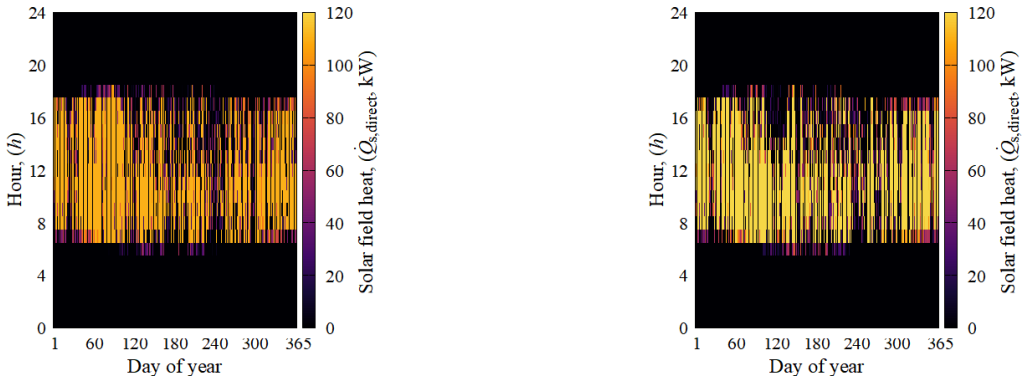

(a) Almoloya del Río (b) Toluca

Figure. 3. *Seasonal distribution of direct solar heat delivery.*

The exergy analysis provides a more discriminating assessment of the system's thermodynamic performance than energy metrics alone. At Almoloya del Río, the exergy delivered to the process from direct solar and TES sources amounts to 89.971 MWh and 2.358 MWh respectively, against a total process exergy demand of 243.766 MWh. This yields an exergy-based solar fraction of 37.9%. Notably, this value exceeds the corresponding energy-based solar fraction of 33.4%, indicating that the solar-derived heat is delivered at a thermodynamic quality proportionally higher than its energy share alone would suggest. This outcome is consistent with the operating temperature range of the HTF (140–240°C), which imparts a relatively high Carnot factor to the solar thermal stream relative to the process steam conditions.

At Toluca, the exergy-based solar fraction of 29.5% is conversely lower than the energy-based value of 31.6%. This inversion warrants careful interpretation. It reflects the fact that, at this site, a larger share of the process exergy demand is met by the auxiliary boiler, whose contribution at high flame temperatures carries a comparatively large exergy content that inflates the denominator of the exergy fraction. The result highlights a key advantage of exergy analysis: it reveals thermodynamic nuances that energy-only metrics may obscure.

The time-averaged total energy efficiency $\bar{\eta}_{\mathrm{I,tot}}$ is 0.635 at Almoloya del Río and 0.655 at Toluca. The higher value at Toluca reflects the fact that this site operates closer to its design point for a greater proportion of the

year, with correspondingly less auxiliary fuel consumption relative to total solar input. The time-averaged total exergy efficiency $\bar{\eta}_{\mathrm{II,tot}}$ is 0.2 at Almoloya del Río and 0.258 at Toluca. These values are characteristic of PTC-based SHIP systems operating at intermediate temperatures, wherein significant exergy destruction occurs in the heat exchange process between the HTF and the steam header, as well as within the thermocline storage unit.

Figures 4a and 4b present heatmaps showing the hourly distribution of both $\eta_{\mathrm{I,tot}}$ and $\eta_{\mathrm{II,tot}}$ across the year for Almoloya del Río; Figures 5a and 5b present the corresponding data for Toluca. The energy efficiency heatmaps reveal relatively stable performance during operating hours, with the highest values concentrated in mid-morning to early afternoon periods coinciding with peak irradiance. The exergy efficiency heatmaps exhibit greater variability, with lower values observed during transient periods at the margins of the solar window. In these marginal periods, partial-load operation and heat exchanger mismatching reduce the thermodynamic quality of the delivered heat stream. These patterns are consistent across both sites, though the Toluca figures display a more pronounced midday peak owing to the site's higher design-point irradiance.

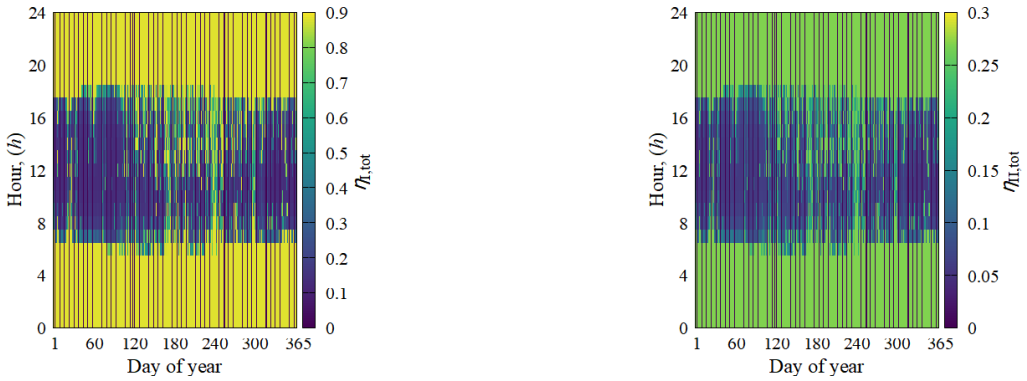

(a) Energy efficiency (b) Exergy efficiency

Figure. 4. *Total efficiency for Almoloya del Río.*

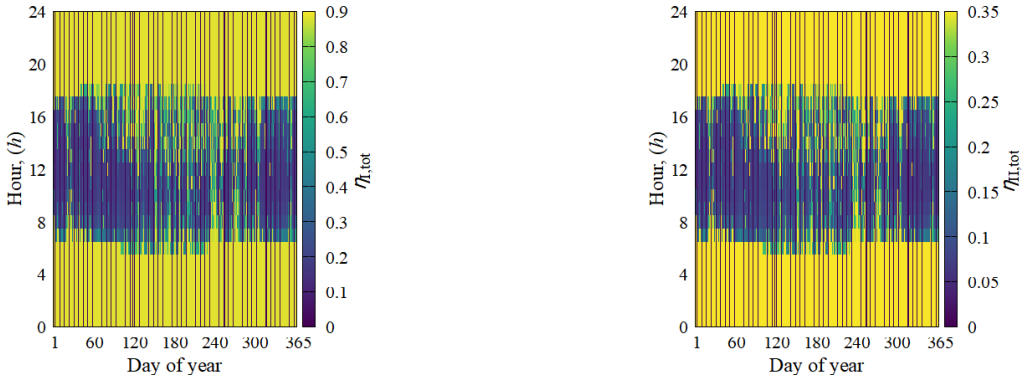

(a) Energy efficiency (b) Exergy efficiency

Figure. 5. *Total efficiency for Toluca.*

The integration of the solar field yields substantial reductions in natural gas consumption at both sites. Without solar assistance, each factory consumes approximately 54.7–55 tons of natural gas annually to meet the full process heat demand. With the SHIP system in operation, consumption falls to 27.359 tons per year at Almoloya del Río, representing a fuel saved fraction of 50.0% and an annual reduction of approximately 27.331 tons. At Toluca, the savings are even more pronounced, with consumption reduced to 9.3 tons per year—a fuel saved fraction of 83.1% and an annual saving of approximately 45.691 tons. The markedly higher fuel saved fraction at Toluca reflects the combination of a larger nominal solar contribution, a higher solar multiple, and a more favourable local irradiance regime. Collectively, these factors enable the solar field and thermal energy storage unit to satisfy a greater proportion of the process load throughout the year.

These fuel savings translate directly into significant reductions in operating expenditure. The annual natural gas cost without solar integration amounts to US$8174.24 per factory at both sites, consistent with the identical process demand and fuel tariff structure. With the SHIP system, annual fuel costs reduce to US$4119.32 at Almoloya del Río and US$1415.11 at Toluca, representing cost savings of US$4054.92 and US$6759.13 per year respectively.

Figures 6a and 6b present the monthly breakdown of fuel costs for both the baseline and solar-assisted scenarios, for Almoloya del Río and Toluca respectively. These bar charts reveal a clear seasonal pattern in

the magnitude of savings. Both sites exhibit the largest cost differentials during the spring and summer months, particularly between May and September. During this period, beam normal irradiance reaches its annual peak, and the solar field operates at or near its design output for the greatest number of hours per day. Conversely, the winter months of November through January show the smallest absolute savings, reflecting reduced solar availability and the correspondingly greater reliance on auxiliary fuel. The Toluca charts are particularly striking. Several summer months, most notably September, show near-zero fuel costs under solar-assisted operation. This confirms that the system can approach full solar coverage of the daily process load during optimal irradiance conditions.

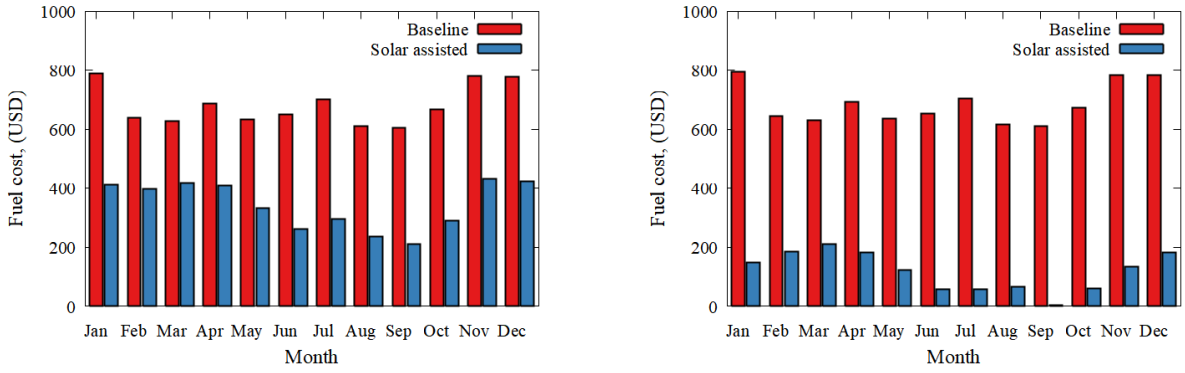

(a) Almoloya del Río (b) Toluca

Figure. 6. *Fuel costs.*

Table 3 consolidates the key performance indicators for both sites, enabling a structured cross-site comparison. Whilst the two installations share an identical hardware configuration, the results demonstrate that site-specific meteorological conditions exert a measurable influence on all performance dimensions. Toluca consistently outperforms Almoloya del Río in terms of absolute solar delivery, fuel displacement, and cost savings. This advantage is attributable to its marginally superior beam normal irradiance resource and higher design-point nominal contribution. However, Almoloya del Río achieves a higher energy-based solar fraction and a higher exergy-based solar fraction, reflecting the fact that its lower process demand is proportionally better matched by the fixed collector array capacity.

The exergy efficiencies of 16.3% and 22.9% at Almoloya del Río and Toluca, respectively, whilst modest, are consistent with the broader literature on PTC-based SHIP systems operating at sub-250°C temperatures. The analysis identifies the principal sources of exergy destruction as the heat exchange process between the HTF and the steam header—where temperature mismatching introduces irreversibility—and the thermocline storage unit, where thermal stratification degradation over charge–discharge cycles reduce the effective quality of stored energy. These findings suggest that future design iterations should prioritise heat exchanger optimisation and explore stratified multi-node storage configurations. Such improvements offer pathways to enhancing second-law performance without expanding the collector area.

Taken together, the results confirm that PTC-based SHIP is thermodynamically and operationally viable under the rooftop spatial constraints characteristic of denim manufacturing facilities in the Toluca Valley. Meaningful fuel savings and cost reductions are achievable even when the solar fraction remains constrained to the 30–34% range by the available installation area.

4. Conclusions

This study aimed to evaluate the technical, thermodynamic, and environmental performance of a roof-mounted parabolic trough collector-based Solar Heat for Industrial Processes (SHIP) system serving denim manufacturing facilities in the Toluca Valley, México, under realistic rooftop spatial constraints. To achieve this, we developed and applied a validated, non-iterative thermohydraulic model coupled with first- and second-law analyses conducted on an hourly basis. The methodology integrated site-specific meteorological data, a constrained-area collector sizing procedure, and a thermocline thermal energy storage unit designed with a solar multiple of 1.5.

The results demonstrate that the proposed SHIP configuration achieves solar fractions of 33.4% and 31.6% at Almoloya del Río and Toluca respectively. These systems displace between 50% and 83% of the annual natural gas consumption relative to a boiler-only baseline, generating annual fuel cost savings of US$4,055 and US$6,759 per factory. The exergy analysis reveals time-averaged second-law efficiencies of 16.3% and 22.9% at the two sites, confirming that heat exchanger temperature mismatching and thermocline storage degradation represent the dominant sources of irreversibility within the integrated system. We further demonstrate that the exergy-based solar fraction diverges meaningfully from its energy-based counterpart—

exceeding it at Almoloya del Río yet falling below it at Toluca. This finding underscores the necessity of second-law assessment in correctly characterising the thermodynamic quality of solar-derived process heat.

We acknowledge several limitations. The single-node thermocline storage model and the assumption of steady-state boiler efficiency introduce simplifications that may moderately overestimate storage exergy retention and auxiliary thermal output under highly transient operating conditions. Additionally, restricting the analysis to two sites, whilst representative of the regional denim industry cluster, limits the immediate generalisability of the quantitative results to facilities with substantially different rooftop geometries or process schedules.

These findings advance the existing literature by providing the first exergy-focused, area-constrained assessment of PTC-based SHIP for the Mexican textile sector. Prior studies have addressed this context only through energy-level techno-economic screening without spatial or second-law rigour. The demonstrated viability of meaningful solar fractions within a sub-1000 m² rooftop envelope directly challenges the prevailing assumption that PTC-based industrial solar heat is impractical for facilities with limited installation area. This work offers a replicable design methodology transferable to analogous industrial clusters across Latin America.

Future research should prioritise multi-node storage models, or those resolved with computational fluid dynamics, to better quantify exergy destruction within the thermocline unit. Investigators should also explore dynamic HTF flow control strategies to reduce heat exchanger irreversibility during off-design operating conditions. Furthermore, extending the present framework to incorporate a life-cycle carbon assessment and a full techno-economic optimisation—including collector orientation, storage capacity, and solar multiple as simultaneous decision variables—would provide a more complete basis for investment decision-making in the regional industrial sector.

Acknowledgments

The authors acknowledge the Consejo Mexiquense de Ciencia y Tecnología (COMECyT) for supporting EGM through the 'Investigadoras e Investigadores COMECyT' programme. This research, conducted within the framework of the AESCo project, utilised the resources and funding provided by this initiative to achieve its objectives.

Nomenclature

Example:

c specific heat, kJ/(kg K)

CF capacity factor

ex specific exergy, kJ/kg

FSF fuel saved fraction

K thermal load fraction

$\dot{m}$ mass flow rate, kg/s

$\dot{Q}$ thermal power, kW

SF Solar fraction

SM Solar multiple

T temperature, °C

Greek symbols

η efficiency

φ maintenance factor

Subscripts and superscripts

I first law

II second law

direct direct

References

[1] Vesely L, Rapp L, Kapat J. Techno-Economic Evaluation of Waste Heat Recovery Systems for Industrial Decarbonization. J Eng Gas Turbine Power 2026;148. https://doi.org/10.1115/1.4069790.

[2] Turchetti L. Preface: SolarPACES 2024, 30th International Con-ference on Concentrating Solar Power, Thermal, and Chemical Energy Systems. SolarPACES Conference Proceedings 2025;3. https://doi.org/10.52825/solarpaces.v3i.2884.

[3] Liaqat K, Schulke G, Schaefer L. Feasibility Analysis of Implementing Small-Scale CSP System for Industrial Process Heat on Urban Brownfields. ASME 2025 19th International Conference on Energy Sustainability, American Society of Mechanical Engineers; 2025. https://doi.org/10.1115/ES2025-156769.

[4] Marzouk OA. Solar Heat for Industrial Processes (SHIP): An Overview of Its Categories and a Review of Its Recent Progress. Solar 2025;5:46. https://doi.org/10.3390/solar5040046.

[5] Catarino ML, Sampaio F, Gonçalves AL. Sustainable Wet Processing Technologies for the Textile Industry: A Comprehensive Review. Sustainability 2025;17:3041. https://doi.org/10.3390/su17073041.

[6] Santana JP, Arto Delgado A, Climente García A, Acosta-Pazmiño I, Gomes J. Evaluating the Potential of Solar Heat Production for the Food and Beverage Industry in Cyprus From 2024 to 2035. SolarPACES Conference Proceedings 2025;3. https://doi.org/10.52825/solarpaces.v3i.2393.

[7] Kumar L, Hasanuzzaman M, Rahim NA, Sleiti AK. Thermoeconomic Analysis of a Solar-Assisted Industrial Process Heating System. Int J Energy Res 2024;2024. https://doi.org/10.1155/2024/4614066.

[8] Nájera-Trejo M, Álvarez-Chavarría F, Rodríguez-Muñoz NA, Romero-Pérez CK, Martín-Domínguez IR, Ortega-Avila N. Pre-Feasibility Assessment Tool for Solar Industrial Process Heating. Processes 2023;11:1663. https://doi.org/10.3390/pr11061663.

[9] Ortiz-Guerrero N, González-López R. Multilevel and Multiregional Analysis of the Electricity Metabolism of Mexico across Sectors. Electricity 2023;4:1–21. https://doi.org/10.3390/electricity4010001.

[10] Catarino ML, Sampaio F, Gonçalves AL. Sustainable Wet Processing Technologies for the Textile Industry: A Comprehensive Review. Sustainability 2025;17:3041. https://doi.org/10.3390/su17073041.

[11] Pérez-Hernández CC, Salazar-Hernández BC, Mendoza-Moheno J, Cruz-Coria E, Hernández-Calzada MA. Mapping the Green Product-Space in Mexico: From Capabilities to Green Opportunities. Sustainability 2021;13:945. https://doi.org/10.3390/su13020945.

[12] Espino-Reyes CA, Ortega-Avila N, Rodriguez-Muñoz NA. Energy Savings on an Industrial Building in Different Climate Zones: Envelope Analysis and PV System Implementation. Sustainability 2020;12:1391. https://doi.org/10.3390/su12041391.

[13] Comisión Nacional de Energía. Índices de Referencia de Precios de Gas Natural 2026. https://www.cne.gob.mx/ipgn/ (accessed March 11, 2026).

[14] Therminoil. Therminol Heat Transfer Fluids by Eastman 2020. https://www.therminol.com (accessed September 17, 2020).

[15] Inventive Power. POWER TROUGH 250 2013. https://inventivepower.com.mx/solucion-en-energia-solar/power-trough-250/ (accessed January 3, 2024).

[16] González-Mora E, Durán-García MD. Alternative Approach for Thermo-Hydraulic Modeling of Direct Steam Generation in Parabolic Trough Solar Collectors. J Therm Sci Eng Appl 2024;16:1–12. https://doi.org/10.1115/1.4064819.

[17] González-Mora E. A RATIONAL EFFICIENCY DEFINITION FOR HEAT EXCHANGERS. System Research in Energy 2025;2025:123–34. https://doi.org/10.15407/srenergy2025.04.123.

[18] González-Mora E, Poudel R, Durán-García MD. A practical upper-bound efficiency model for solar power plants. Journal of Non-Equilibrium Thermodynamics 2023. https://doi.org/10.1515/jnet-2022-0080.

[19] Szargut J. Exergy method: technical and ecological applications. vol. 18. WIT press; 2005.